Emission spectra of quasimetastable levels of alkali-metal atoms

A. J. Mendelsohn,* C. P. J. Barty, M. H. Sher, J. F. Young, and S. E. Harris
Edward L. Ginzton Laboratory, Stanford University, Stanford, California 94305
(Received 30 September 1985; revised manuscript received 7 November 1986)

The paper describes the experimental investigation of a subclass of quartet levels of the alkali-metal atoms which retain metastability against autoionization and have large radiative yields. Using high-pulsed-power microwaves, we obtain emission spectra of Na, K, Rb, and Cs. In each case, the neutral emission spectrum is dominated by emission from these levels.

I. INTRODUCTION

It is well known that the quartet level of highest J of a given configuration of an alkali-metal atom is metastable against both autoionization and radiation in the extreme-ultraviolet (xuv) region. This occurs since, irrespective of the extent to which LS coupling holds, there is no doublet level in the configuration to which the quartet level may couple. The autoionization or radiative decay of such a quartet level requires a change of electron spin and is therefore quite slow. For example, the $3p^5 3d\,4s\ ^4F_{9/2}$ level of K has a measured[1] autoionizing lifetime of 90 μs.

It has recently been noted that there exists a subclass of quartet levels which retains relative metastability against autoionization, and which also radiates in the extreme-ultraviolet region.[2] The distinguishing property of these quartets is that the selection rules for spin-orbit matrix elements allow nonzero matrix elements only to doublet basis levels which, due to angular momentum and parity considerations, are themselves prohibited from autoionizing but are radiatively allowed to decay. Such quartet levels have been termed "quasimetastable." For alkali-metal atoms, the condition for quasimetastability is that a level have parity and orbital angular momentum that are both odd or both even, that $|J-L|=\frac{3}{2}$, and that the level not be a pure (highest J) quartet.

An example of a quasimetastable level is the $3p^5 3d\,4s\ ^4P_{5/2}$ level of K. The calculated autoionizing and radiative lifetimes for this level are 5.56 and 0.29 μs, respectively. Figure 1 is an energy-level diagram showing the radiative decay from this level to a valence level of the atom.

For each of the alkali-metal elements other than Li, the lowest level of the quartet manifold is quasimetastable rather than metastable. Since it radiates in the xuv region, it may be used to determine the position of the quartet manifold relative to the ground level of the atom. Laser-induced fluorescence,[3] or laser-caused depletion of the radiation from the quasimetastable level,[4] may then be used to determine other levels of the quartet manifold.

Quasimetastable levels of alkali-metal elements may be used in the construction of xuv lasers in two ways. In Na and K, the admixture of nonautoionizing doublet levels with the quasimetastable quartets allows population stored in quasimetastable levels to be transferred to radiating doublet levels using several orders of magnitude less transfer laser power than does an earlier proposed[5] system in Li. In the heavier alkali metals, the Einstein A coefficients for xuv emission are sufficiently large that laser emission should be obtainable on transitions from the quasimetastable level to a valence level of the atom.

This paper describes the results of a set of experiments in which a high-power (500-kW) X-band microwave discharge source was used to take the emission spectra of Na, K, Rb, and Cs. Emission wavelengths, intensities relative to the inert-gas-like ion lines, and, in some cases, fine-structure splittings are noted. The experimental results are striking. In each case, emission from either of the two lowest quasimetastable levels dominates the neutral spectrum. In Rb the intensity of the quasimetastable emission is about one-fourth that of the strongest ion line.

II. QUASIMETASTABILITY

In an alkali-metal-atom configuration in which LS coupling is a good approximation, two classes of levels are metastable against autoionization. The first is the class of quartet levels which lie below the lowest triplet level of

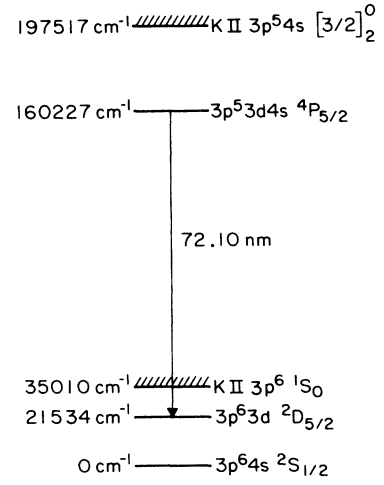

FIG. 1. Energy-level diagram showing the $3p^5 3d\,4s\ ^4P_{5/2}$ level of K.

TABLE I. Radiative and autoionizing rates for levels of the K $3p^5 3d\,4s$ configuration.

Level	Radiative rate (s^{-1})	Autoionizing rate (s^{-1})	Type of level
$^4P_{5/2}$	3.5×10^6	1.8×10^5	Quasimetastable quartets
$^4F_{3/2}$	1.2×10^7	3.7×10^6	
$^4P_{1/2}$	2.8×10^6	1.5×10^{10}	Other quartets
$^4P_{3/2}$	7.2×10^6	2.6×10^{10}	
$^4D_{1/2}$	1.8×10^7	3.2×10^{11}	
$^4D_{3/2}$	5.9×10^7	9.8×10^{10}	
$^4D_{5/2}$	9.5×10^7	4.5×10^{11}	
$^4D_{7/2}$	6.0×10^7	1.1×10^{11}	
$^4F_{5/2}$	3.4×10^7	2.9×10^{11}	
$^4F_{7/2}$	3.3×10^7	3.7×10^{11}	
$^4F_{9/2}$			Metastable quartet
$(^1D)^2D_{3/2}$	4.9×10^8	1.6×10^{11}	Nonautoionizing doublets
$(^3D)^2D_{3/2}$	1.1×10^9	6.3×10^9	
$(^1D)^2D_{5/2}$	3.2×10^8	5.2×10^{11}	
$(^3D)^2D_{5/2}$	1.2×10^9	3.9×10^{11}	
$(^1P)^2P_{1/2}$	3.0×10^{10}	1.0×10^{14}	Autoionizing doublets
$(^3P)^2P_{1/2}$	7.9×10^8	1.8×10^{13}	
$(^1P)^2P_{3/2}$	2.6×10^{10}	9.1×10^{13}	
$(^3P)^2P_{3/2}$	8.2×10^8	1.7×10^{13}	
$(^1F)^2F_{5/2}$	2.0×10^8	4.9×10^{10}	
$(^3F)^2F_{5/2}$	1.0×10^9	1.8×10^{13}	
$(^1F)^2F_{7/2}$	3.7×10^8	7.3×10^{10}	
$(^3F)^2F_{7/2}$	8.3×10^8	1.9×10^{13}	

the ion. These levels are metastable by the requirement of conservation of spin. The second is the class of doublet levels which have even parity and odd orbital angular momentum, or odd parity and even orbital angular momentum; these quantities cannot be simultaneously conserved during Coulombic autoionization.

Within a single configuration, breakdown of LS coupling causes mixing of doublet and quartet levels of a given J. The spin-orbit interaction term $\mathbf{L}\cdot\mathbf{S}$ connects pure LS basis levels satisfying $\Delta L=0,\pm1$; $\Delta S=0,\pm1$, and $\Delta J=0$. This mixing causes doublets, which are forbidden to autoionize by parity and angular momentum, to mix with doublets that do autoionize; consequently, in the heavier alkali metals, all doublets tend to autoionize. Similarly, except for the quartet of highest J, the quartets also mix with autoionizing doublets and therefore autoionize.

These ideas are illustrated in Table I for the $3p^5 3d\,4s$ configuration of K. The table shows the radiative and autoionizing rate for each class of level in the configuration. The values were calculated with the *RCN/RCG* atomic physics code developed by Cowan[6] including the $3p^5 4s^2$, $3p^5 3d\,4s$, $3p^5 4s\,5s$, $3p^5 4p^2$, and $3p^5 3d^2$ configurations. The term "nonautoionizing" doublet in Table I refers to those doublet levels which, if pure, would not autoionize. The breakdown in LS coupling causes these doublets, as well as most of the quartets, to autoionize. The level with the highest radiative yield, and also the lowest level in the quartet manifold is the $3p^5 3d\,4s\ ^4P_{5/2}$ quasimetastable.

The *RCN/RCG* eigenvector expansion of this level is

$$
\begin{aligned}
3p^5 3d\,4s\ ^4P_{5/2} = {} & 0.994(3p^5 3d\,(^3P)4s\ ^4P_{5/2}) - 0.067(3p^5 3d\,(^3D)4s\ ^4D_{5/2}) + 0.056(3p^5 3d\,(^1D)4s\ ^2D_{5/2}) \\
& + 0.029(3p^5 3d\,(^3D)4s\ ^2D_{5/2}) + 0.001(3p^5 3d\,(^3F)4s\ ^4F_{5/2}) - 0.0002(3p^5 3d\,(^1F)4s\ ^2F_{5/2}) \\
& + 0.000\,07(3p^5 3d\,(^3F)4s\ ^2F_{5/2}) - 0.016(3p^5 4s\,(^3P)5s\ ^4P_{5/2}) + 0.008(3p^5 4p\,(^3P)4p\ ^4P_{5/2}) \\
& - 0.0006(3p^5 4p\,(^1D)4p\ ^2D_{5/2}) + 0.0002(3p^5 4p\,(^3D)4p\ ^2D_{5/2}) + 0.043(3p^5 3d\,(^3P)3d\ ^4P_{5/2}) \\
& + 0.003(3p^5 3d\,(^3F)3d\ ^4D_{5/2}) - 0.002(3p^5 3d\,(^3F)3d\ ^2D_{5/2}) + 0.0009(3p^5 3d\,(^3P)3d\ ^4D_{5/2}) \\
& + 0.0008(3p^5 3d\,(^1D)3d\ ^2D_{5/2}) + 0.018(3p^5 3d\,(^3P)5s\ ^4P_{5/2}) - 0.001(3p^5 3d\,(^3D)5s\ ^4D_{5/2}) \\
& + 0.0005(3p^5 3d\,(^1D)5s\ ^2D_{5/2}) - 0.0002(3p^5 3d\,(^3D)5s\ ^2D_{5/2})\ .
\end{aligned}
$$

TABLE II. Quasimetastable quartet levels of alkali-metal-like configurations.

Configuration	Quasimetastable levels	Metastable levels
p^5sp	$^4S_{3/2}$, $^4D_{1/2}$	$^4D_{7/2}$
p^5sd	$^4P_{5/2}$, $^4F_{3/2}$	$^4F_{9/2}$
p^5pd	$^4S_{3/2}$, $^4D_{1/2}$, $^4D_{7/2}$, $^4G_{5/2}$	$^4G_{11/2}$
p^5p^2	$^4P_{5/2}$	
p^5d^2	$^4P_{5/2}$, $^4F_{3/2}$, $^4F_{9/2}$	

TABLE III. Radiative and autoionizing rates for the lowest quasimetastable levels of the alkali metals.

Level	Autoionizing rate (s^{-1})	Radiative rate (s^{-1})
Na $2p^53s\,3p\,^4S_{3/2}$	6.8×10^5	9.7×10^6
K $3p^53d\,4s\,^4P_{5/2}$	1.8×10^5	3.5×10^6
Rb $4p^55s\,5p\,^4S_{3/2}$	8.5×10^7	2.6×10^7
Cs $5p^55d\,6s\,^4P_{5/2}$	1.0×10^8	5.4×10^7

Note that neither the quartet nor the odd angular momentum, even parity doublet basis levels on the right side of the expansion cause autoionization. The autoionizing rate of 1.8×10^5 s^{-1} (Table I) results from the weak (0.0002) second-order coupling of the $^2F_{5/2}$ level. The stronger (0.056) and (0.029) coupling to the (nonautoionizing) $^2D_{5/2}$ levels results in the 3.5×10^6 s^{-1} radiative rate and, therefore, in the large branching ratio for xuv radiation. This coupling to a nonautoionizing doublet is the key idea of quasimetastability.

Table II summarizes the metastable and quasimetastable levels of all s,p,d configurations of the alkali-metal atoms. As noted earlier, the condition for quasimetastability is that $|J-L|=\frac{3}{2}$, that parity and angular momentum be both even or both odd, and that the level not have the highest J in the configuration. This selection rule for quasimetastability is weak and holds best for lower levels such as $^4S_{3/2}$ and $^4P_{5/2}$ which have the greatest energy separation from their neighbors and which, therefore, have the weakest coupling to autoionizing doublets. The selection rule will also fail if configuration interaction mixes in levels which autoionize. For the lower quasimetastable levels of the alkali-metal atoms, such mixing usually does not occur.

Table III gives the autoionizing and radiative rates for the lowest quasimetastable level of each parity for each of the alkali-metal elements except Li. Table IV gives the *RCN/RCG* eigenvector expansion for each of these levels. In this table we only show basis levels belonging to the dominant configuration. Table V summarizes the parameters used in each of the *RCN/RCG* calculations presented.

III. MICROWAVE-EXCITATION APPARATUS

A schematic of the experimental apparatus used in this work is shown in Fig. 2. The emission cell consisted of a stainless-steel X-band waveguide which was internally tapered to a 7.5-cm-long ridge having a 2.5-cm width and a ridge-to-waveguide wall spacing of 2 mm. Microwave power was supplied by a Varian SFD-303 coaxial magnetron with a peak power of 300 kW at 9.375 GHz, a 2-μs pulse length, and a repetition rate of 200 Hz. The metal vapor of each of the alkali metals to be examined was introduced into the region above the ridge by five 2-mm-diam holes which connected this region to a heated reservoir containing the metal. The temperature of the reservoir was adjusted so that the vapor pressure in the cell was between 10^{14} and 10^{15} atoms/cm^3.

The emission spectra were taken with a McPherson Model 225, 1 m, normal incidence monochromator with a 1200-line/mm platinum-coated grating. Because of the low vapor pressure in the cell, no window was needed between it and the monochromator, which was maintained at about 10^{-7} Torr. xuv photons were detected with an EMI Model 7265B electron multiplier. The photoelectrons were amplified, discriminated, counted, and sent to a microcomputer system for data reduction. The counting electronics were enabled only during the microwave pulse.

IV. EMISSION SPECTRA

The xuv emission spectra of Na, K, Rb, and Cs are shown in Fig. 3. In each case the scan was started at the strong (inert-gas-like) ion resonances. These lines were used for wavelength calibration and also to establish the relative excitation efficiency of the neutral lines. The principal result is that all of the observed lines which are associated with the neutral species originate from the quasimetastable levels described in this paper; in addition, these levels are excited and radiate at an efficiency that is often within a factor of 10 of the strongest ion line. Table VI lists the observed transition wavelengths, upper- and lower-level designations, and relative intensity (each ele-

TABLE IV. *RCN/RCG* eigenvector expansion of the lowest quasimetastable levels of the alkali metals.

Level	Expansion
Na $2p^53s\,3p\,^4S_{3/2}$	$=0.982\,^4S-0.137\,^4P+0.066(^1P)^2P+0.042(^3P)^2P$ $+0.006\,^4D-0.001(^1P)^2D-0.0007(^3P)^2D$
K $3p^53d\,4s\,^4P_{5/2}$	$=0.994\,^4P-0.067\,^4D+0.056(^1D)^2D+0.029(^3D)^2D$ $+0.001\,^4F-0.0002(^1F)^2F+0.000\,07(^3F)^2F$
Rb $4p^55s\,5p\,^4S_{3/2}$	$=0.901\,^4S-0.324\,^4P+0.152(^1P)^2P+0.035\,^4D$ $+0.091(^3P)^2P-0.004(^1P)^2D-0.002(^3P)^2D$
Cs $5p^55d\,6s\,^4P_{5/2}$	$=0.889\,^4P-0.349\,^4D+0.233(^1D)^2D+0.131(^3D)^2D$ $+0.052\,^4F+0.003(^1F)^2F-0.0007(^3F)^2F$

TABLE V. Parameters for *RCN/RCG* calculations.

Element	Valence configurations	Core-excited configurations	Free-electron energies (Ry) and angular momenta	Scaling factors
Na	$2p^6 3s$	$2p^5 3s\,3p$	$2.03s,d$	$F^k(i,i)-0.82$
	$2p^6 4s$	$2p^5 3s\,4p$	$2.23s,d$	$F^k(i,j)-0.82$
	$2p^6 3d$	$2p^5 3p\,4s$	$1.85p$	$G^k(i,j)-0.72$
	$2p^6 4d$	$2p^5 3d\,3p$	$2.22p,f$	$R^k(i,j)-0.77$
	$2p^6 3p$	$2p^5 3s^2$	$2.32p,f$	$\zeta_i-1.00$
	$2p^6 4p$	$2p^5 3d\,3s$		
		$2p^5 3s\,4s$		
		$2p^5 3s\,4d$		
		$2p^5 3s\,5d$		
K	$3p^6 4s$	$3p^5 4s\,4p$	$1.20s,d$	$F^k(i,i)-0.77$
	$3p^6 3d$	$3p^5 4s\,5p$	$1.37s,d,g$	$F^k(i,j)-0.77$
	$3p^6 4d$	$3p^5 3d\,4p$	$1.08p$	$G^k(i,j)-0.77$
	$3p^6 4p$	$3p^5 4s^2$	$1.24p,f$	$R^k(i,j)-0.77$
	$3p^6 5p$	$3p^5 3d\,4s$	$1.33p,f$	$\zeta_i-1.00$
		$3p^5 4s\,5s$	$1.43p,f$	
		$3p^5 4p^2$		
		$3p^5 3d^2$		
Rb	$4p^6 5s$	$4p^5 5s\,5p$	$0.98s,d$	$F^k(i,i)-0.77$
	$4p^6 4d$	$4p^5 5s\,6p$	$1.15s,d$	$F^k(i,j)-0.77$
	$4p^6 5d$	$4p^5 4d\,5p$	$0.87p$	$G^k(i,j)-0.77$
	$4p^6 5p$	$4p^5 5s^2$	$1.01p,f$	$R^k(i,j)-0.77$
	$4p^6 6p$	$4p^5 4d\,5s$	$1.19p,f$	$\zeta_i-1.00$
		$4p^5 5s\,6s$		
		$4p^5 5d\,5s$		
		$4p^5 4d^2$		
		$4p^5 5p^2$		
Cs	$5p^6 6s$	$5p^5 6s\,6p$	$0.79s,d$	$F^k(i,i)-0.77$
	$5p^6 7s$	$5p^5 5d\,6p$	$0.88s,d,g$	$F^k(i,j)-0.77$
	$5p^6 5d$	$5p^5 4f\,6s$	$0.97d,g$	$G^k(i,j)-0.77$
	$5p^6 6p$	$5p^5 6s^2$	$0.74p,f$	$R^k(i,j)-0.77$
	$5p^6 4f$	$5p^5 5d^2$	$0.93p,f$	$\zeta_i-1.00$
		$5p^5 5d\,6s$		
		$5p^5 6s\,7s$		

ment normalized only to itself and its ions) of each of the observed quasimetastable lines. Table VII lists the other lines observed in the scans.

The identifications in Table VI are based on several factors. These include (1) the wavelength and branching ratio for radiation (as opposed to autoionization) as predicted by the *RCN/RGN* atomic physics code; (2) the observation of the emission doublets which result from the fine structure of the lower level of the xuv transition and the comparison of the experimental and theoretical ratio of the intensities of its components; (3) the observation of emission series which correspond to p^6nl configurations in the valence manifold; and (4) the identification of other workers based on absorption, emission, or ejected electron spectroscopy.

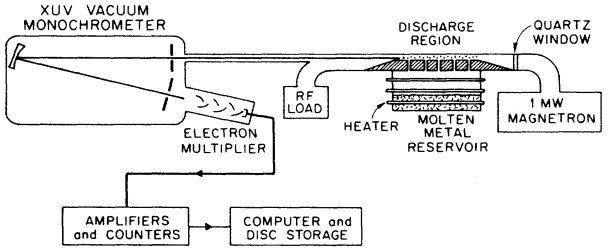

FIG. 2. Microwave excitation apparatus.

The emission spectrum of Na is particularly simple. The primary neutral line at 40.52 nm originates from the $2p^5 3s\,3p\ ^4S_{3/2}$ level and terminates on the $2p^6 3p\ ^2P_{1/2,3/2}$ levels. This line was previously observed in a low-resolution emission spectrum taken by Zhemenyak *et al.*,[7] and in ejected electron spectra by Pegg *et al.*[8]

In K the emission spectrum is dominated by transitions which originate from two quasimetastable levels, both of which have been noted earlier by Aleksakhin *et al.*[9] The lowest of these levels is $3p^5 3d\,4s\ ^4P_{5/2}$ at an energy of 160 227 cm^{-1} which radiates to the $3p^6 3d\ ^2D_{3/2,5/2}$ valence levels at 72.10 nm. The other quasimetastable level is $3p^5 4s\,4p\ ^4S_{3/2}$ at an energy of 161 426 cm^{-1}. Its

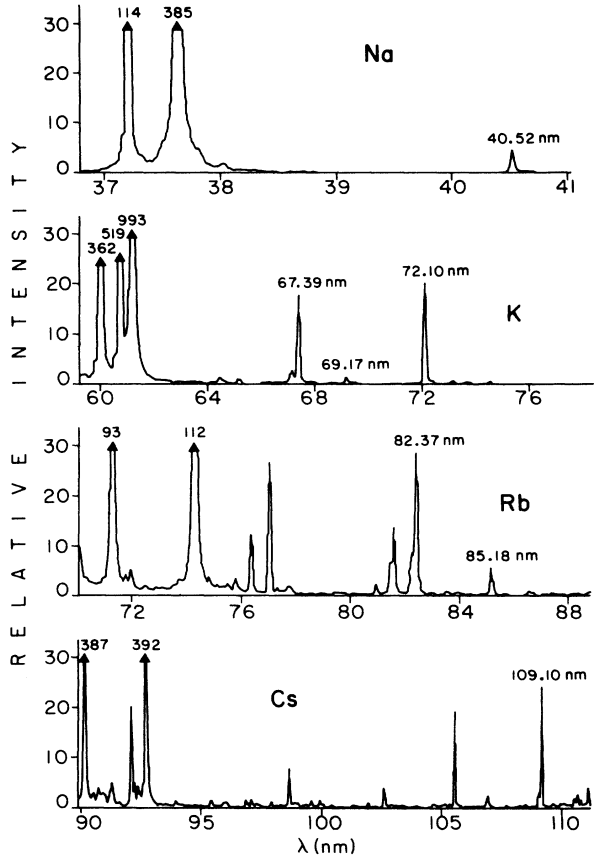

FIG. 3. Emission spectra of the alkali metals.

identification was first made by Mansfield and Ottley[10] on the basis of ejected electron spectroscopy and is confirmed here by the emission doublet at 67.39 and 67.36 nm (Fig. 4) corresponding to the fine-structure splitting of the $3p^6 4p\ ^2P_{1/2,3/2}$ valence levels. The alkali-metal valence

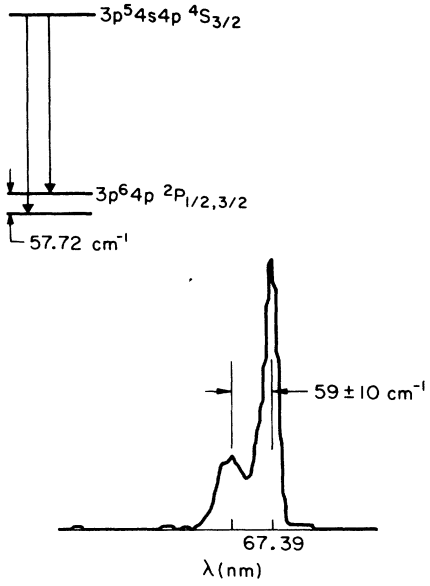

FIG. 4. Fine-structure splitting of the K $3p^5 4s 4p\ ^4S_{3/2} - 3p^6 4p\ ^2P_{1/2,3/2}$ transitions.

level splittings and positions used here are in all cases taken from Moore.[11] In addition, we have identified the weak line at 69.17 nm as the transition from the $3p^5 3d 4s\ ^4F_{3/2}$ quasimetastable level, based on the work of Mansfield and Ottley.[6]

In Rb the $4p^5 5s 5p\ ^4S_{3/2}$ quasimetastable is the lowest level in the quartet manifold with an energy of 134 220 cm^{-1}. The observed emission from this level includes a fine-structure doublet at 82.37 nm (Fig. 5) which has been tentatively identified by Aleksakhin *et al.*[9] and a weak line at 90.53 nm which is due to decay to the $4p^6 6p\ ^2P_{1/2,3/2}$ levels. The emission from $4p^5 4d 5s\ ^4P_{5/2}$ at 85.18 nm is also observed. The identification of this

TABLE VI. Quasimetastable lines observed in microwave-excitation spectra.

Element	Upper level	Lower level	λ[a] (nm)	Relative intensity	Upper-level energy (cm^{-1})	Other experiment (cm^{-1})
Na	$2p^5 3s\ 3p\ ^4S_{3/2}$	$2p^6 3p\ ^2P_{3/2,1/2}$	40.52	7.0	263 789±120	263 887[b]
K	$3p^5 4s\ 4p\ ^4S_{3/2}$	$3p^6 4p\ ^2P_{3/2}$	67.39	23.0	161 426±60	161 473±65[c]
		$3p^6 4p\ ^2P_{1/2}$	67.36	6.0		
	$3p^5 3d\ 4s\ ^4F_{3/2}$	$3p^6 3d\ ^2D_{3/2,5/2}$	69.17	2.0	166 092±60	166 221±65[c]
	$3p^5 3d\ 4s\ ^4P_{5/2}$	$3p^6 3d\ ^2D_{3/2,5/2}$	72.10	27.0	160 227±60	160 245±65[c]
Rb	$4p^5 5s\ 5p\ ^4S_{3/2}$	$4p^6 5p\ ^2P_{3/2}$	82.37	30.0	134 220±40	134 176±295[d]
		$4p^5 5p\ ^2P_{1/2}$	82.20	12.0		
		$4p^6 6p\ ^2P_{3/2,1/2}$	90.53	0.5		
	$4p^5 4d\ 5s\ ^4P_{5/2}$	$4p^6 4d\ ^2D_{5/2,3/2}$	85.18	6.0	136 756±40	136 831±40[e]
Cs	$5p^5 5d\ 6s\ ^4P_{5/2}$	$5p^6 5d\ ^2D_{5/2}$	109.10	24.0	106 256±30	106 490±242[f]
		$5p^6 5d\ ^2D_{3/2}$	108.98	2.0		
		$5p^6 6d\ ^2D_{5/2,3/2}$	119.58	3.0		
		$5p^6 7d\ ^2D_{5/2,3/2}$	124.72	1.0		

[a]Wavelengths are ±0.03 nm.
[b]Reference 7.
[c]Reference 10.
[d]Reference 9.
[e]Reference 12.
[f]Reference 15.

TABLE VII. Other observed lines.

Species	$\lambda_{\text{other expt}}$ (nm)	λ_{obs} (nm)	Relative intensity	Source
Na II	37.2074	37.21	114	Ref. 16
Na II	37.6377	37.64	385	Ref. 16
K II	60.076	60.07	362	Ref. 16
K II	60.793	60.79	519	Ref. 16
K II	61.262	61.26	993	Ref. 16
Rb II	71.182	71.18	93	Ref. 17
Rb II	74.146	74.12	112	Ref. 17
Rb III	76.904	76.90	27	Ref. 17
Rb III	81.528	81.53	15	Ref. 17
Cs II	90.127	90.13	387	Ref. 17
Cs II	92.666	92.69	392	Ref. 17
Cs III	92.035	92.04	20	Ref. 17
Cs III	105.479	105.48	19	Ref. 17

latter line has also been noted by Mansfield[12] and Aleksakhin *et al.*[9]

In Cs the emission from $5p^5 5d\,6s\ ^4P_{5/2}$ at 109.10 nm dominates the neutral spectrum. This line was identified by Holmgren *et al.*[13] who observed the 98-cm^{-1} splitting attributable to the $5d$ lower level (Fig. 6). This line was previously reported to be at 108.5 nm by Aleksakhin *et al.*[9] Emission was also observed at 119.58 and 124.72 nm corresponding to the decay of the $^4P_{5/2}$ level to the $5p^6 6d$ and $5p^6 7d$ lower configurations.

V. SPECTROSCOPIC APPLICATION OF QUASIMETASTABLE LEVELS

This work has established the identification of the lowest quasimetastable levels of each of the alkali-metal elements, and has verified the predictions of an earlier theoretical paper. Because these quasimetastable levels also accumulate substantial population,[14] they may be used as a starting point for the determination of the relative positions and linewidths of much of the core-excited manifold. In one example of this technique, Holmgren *et al.* have used laser-produced fluorescence from population stored in the Na $2p^5 3s\,3p\ ^4S_{3/2}$ level to identify 15 levels and 30 transitions within the Na quarted manifold.[3] In recent work, Spong *et al.* have monitored radiation from the Rb $(4p^5 4s\,2p)^4S_{3/2}$ level at 82.4 nm, while tuning a visible laser to access other levels of the quartet and doublet manifolds.[4] As these levels are accessed, the xuv emission is reduced, thereby determining the position and linewidth of these levels.

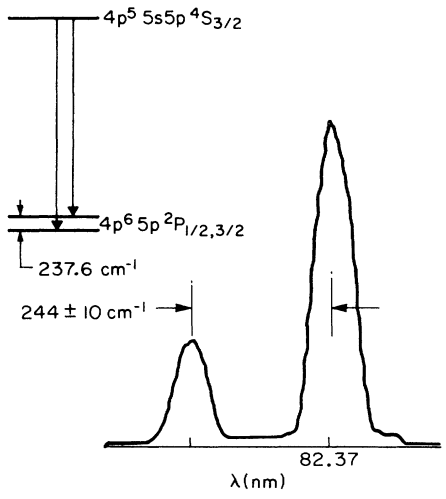

FIG. 5. Fine-structure splitting of the Rb $4p^5 5s\,5p\ ^4S_{3/2} - 4p^6 5p\ ^2P_{1/2,3/2}$ transitions.

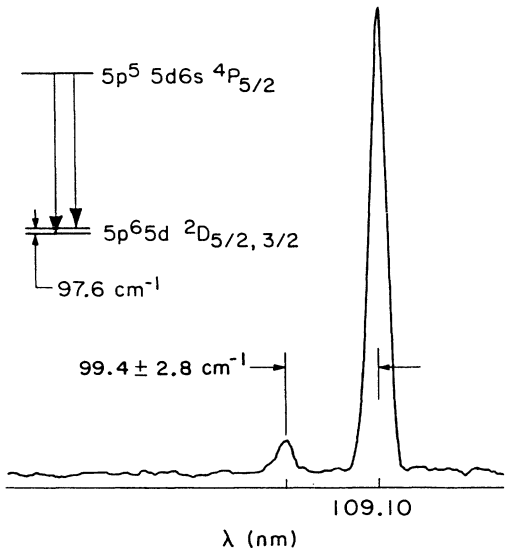

FIG. 6. Fine-structure splitting of the Cs $5p^5 5d\,6s\ ^4P_{5/2} - 5p^6 5d\ ^2D_{5/2,3/2}$ transitions.

ACKNOWLEDGMENTS

The authors acknowledge helpful discussions with R. D. Cowan of the Los Alamos National Laboratory, J. Reader, T. Lucatorto, and A. W. Weiss of the National Bureau of Standards, D. E. Holmgren of the University of Rochester, and with R. G. Caro, K. D. Pedrotti, and D. J. Walker of Stanford University. C. P. J. Barty and M. H. Sher acknowledge, respectively, the support of the Office of Naval Research and of AT&T Bell Labs. The work described here was supported by the Air Force Office of Scientific Research and the Army Research Office.

---

*Present address: Stanford Research Systems, 460 California Avenue, Palo Alto, California 94306.

[1]P. Feldman and R. Novick, Phys. Rev. **160**, 143 (1967).

[2]S. E. Harris, D. J. Walker, R. G. Caro, A. J. Mendelsohn, and R. D. Cowan, Opt. Lett. **9**, 168 (1984).

[3]D. E. Holmgren, D. J. Walker, D. A. King, and S. E. Harris, Phys. Rev. A **31**, 677 (1985).

[4]J. K. Spong, J. D. Kmetec, J. F. Young, and S. E. Harris (unpublished).

[5]S. E. Harris, Opt. Lett. **5**, 1 (1980).

[6]R. D. Cowan, *The Theory of Atomic Structure and Spectra* (University of California Press, Berkeley, California, 1981), Chaps. 8-1, 16-1, and 18-7. The *RCN/RCG* atomic physics code calculates atomic wave functions using the single-configurational Hartree-Fock method, and includes configuration interaction by diagonalization of the interaction Hamiltonian. The inputs to the code are the desired configurations, the energies and angular momenta of the free electrons, and scalar factors for the radial integrals. The code calculates energy eigenvalues, eigenvector expansions, radiative transition probabilities, and autoionizing times. For each of the quoted autoionizing times, we have tested the code for sensitivity to the inclusion of additional configurations.

[7]Yu. U. Zhemanyak, V. S. Vukstich, and I. P. Zapesochnyi, Pis'ma Zh. Eksp. Teor. Fiz. **35**, 321 (1982) [JETP Lett. **35**, 393 (1982)].

[8]D. J. Pegg, H. H. Haselton, R. S. Thoe, P. M. Griffin, M. D. Brown, and I. A. Sellin, Phys. Rev. A **12**, 1330 (1975).

[9]I. S. Aleksakhin, G. G. Bogachev, I. P. Zapesochnyi, and S. Yu. Ugrin, Zh. Eksp. Teor. Fiz. **80**, 2187 (1981) [Sov. Phys.—JETP **53**, 1140 (1981)].

[10]M. W. D. Mansfield and T. W. Ottley, Proc. R. Soc. London, Ser. A **365**, 413 (1979).

[11]C. E. Moore, *Atomic Energy Levels*, Natl. Stand. Ref. Data Ser. (U.S. GPO, Washington, D.C., 1971), Vols. I–III.

[12]M. W. D. Mansfield, Proc. R. Soc. London, Ser. A **364**, 135 (1978).

[13]D. E. Holmgren, D. J. Walker, and S. E. Harris, in *Laser Techniques in the Extreme Ultraviolet*, edited by S. E. Harris and T. B. Lucatorto (AIP, New York, 1984), pp. 496–501.

[14]D. E. Holmgren, R. W. Falcone, D. J. Walker, and S. E. Harris, Opt. Lett. **9**, 85 (1984).

[15]J. P. Connerade, M. W. D. Mansfield, G. H. Newsom, D. H. Tracy, M. A. Baig, and K. Thimm, Philos. Trans. R. Soc. London, Ser. A **290**, 327 (1979).

[16]R. L. Kelly and L. J. Palumbo, *Atomic and Ionic Emission Lines Below 2000 Å—Hydrogen Through Krypton*, Naval Research Laboratory Report No. 7599 (U.S. GPO, Washington, D.C., 1973).

[17]*Handbook of Chemistry and Physics*, 60th ed., edited by R. C. Weast (CRC, Cleveland, Ohio, 1979).